Subsurface Sensing Technologies and Applications Vol. 4, No. 4, October 2003 (©2003)

Medical Imaging Techniques Combining Light and Ultrasound

Charles A. DiMarzio*

Department of Electrical and Computer Engineering, 440 Dana Building, Northeastern University, 360 Huntington Avenue, Boston, MA 02115

Todd W. Murray

Department of Aerospace and Mechanical Engineering, Boston University, 110 Cummington St., Boston, MA 02215

Received September 30, 2002; revised May 28, 2003

The combination of light and ultrasound can lead to new medical imaging techniques combining the spectroscopic capability of light with the spatial resolution of ultrasound. Spectroscopy can be used to measure blood volume and blood oxygen, but because most biological tissues are highly scattering at optical wavelengths, spatial resolution is poor. Ultrasound provides excellent resolution, but not good soft-tissue contrast. There are many techniques for combining light and ultrasound, but the two discussed in this paper have emerged as having the most promise for medical applications. In the first, optoacoustic imaging, an acoustic pulse is generated by a pulse of laser light, and the detected sound is used to produce an image. In the second, acousto-photonic imaging, ultrasound modulates laser light used for diffusive optical tomography. Both of these techniques show promise for a variety of medical applications.

1. Introduction

Sound and light have both found numerous applications in non-invasive medical imaging in recent years. The short wavelength of light permits resolution of sub-cellular features and optical imaging can be used for a range of medical applications including near-surface imaging in dermatology

*To whom all correspondence should be addressed. Phone: 617-373-2034; fax: 617-373-8627; e-mail: dimarzio@ece.neu.edu

1566-0184/03/1000-0289/0

and ophthalmology, where the objects of interest can be seen through transparent media. The importance of light in deep-tissue imaging arises from its spectroscopic capabilities. Chromophores in tissue include hemoglobin (with and without oxygen bound to it), lipids, melanin, water, and beta-carotene. The chromophores of greatest interest are oxygenated and deoxygenated hemoglobin because these are directly related to metabolism. The optical spectra of oxygenated and deoxygenated hemoglobin are different in the near infrared range making it possible to determine the oxygenation state. This information may then be used for functional imaging or for diagnostic purposes to distinguish between benign and malignant tumors. Subsurface optical imaging in tissue is complicated by the fact that near-infrared light, which has relatively low absorption in tissue in comparison to visible light, is nevertheless strongly scattered. Most tissues are optically turbid with scattering arising from inhomogeneities including cellular organelles, extracellular matrices, and membranes. In the early 1990s, new imaging technologies and computational techniques have led to the development of diffusive optical tomography (DOT), for imaging such areas as breast, brain, and fetus *in utero*. By modulating the light source and detecting the amplitude and phase of the modulation, images can be obtained with moderate spatial resolution. Figure 1 gives the dispersion curves for light, diffuse optical waves, and

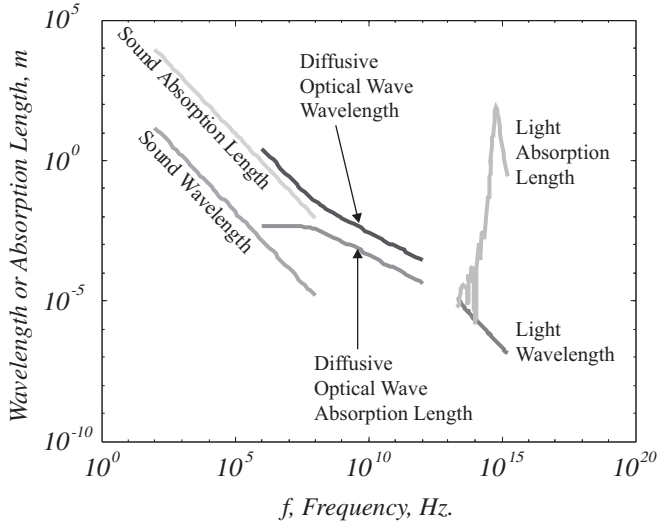

Figure 1. Dispersion curves for various waves. Curves for sound and diffusive waves are shown for typical breast tissue, and values will be somewhat different from one tissue sample to another. The light waves are for a clear medium with an index of refraction of 1.4. Solid lines show wavelength, and dotted lines show absorption length (inverse of absorption coefficient).

ultrasound in soft tissue and shows the limitations and strengths of DOT. The wavelength is significantly longer than that possible with ultrasound or optical imaging in a transparent media, and thus spatial resolution is limited while the absorption length is long so that DOT offers the promise of deep penetration, although the fact that the absorption length is always less than the wavelength limits the ability to resolve small objects at the greater depths.

Ultrasound imaging is a mature technology originally applied to medical applications in the late 1940s and early 1950s. Ultrasound imaging allows us to distinguish changes in the mechanical properties of tissue which result in changes in velocity, attenuation, and scattering of ultrasonic waves. The ultrasonic wavelength determines the spatial resolution and is typically in the range of several hundred microns for ultrasonic frequencies in the low MHz range. Referring to Figure 1, increasing the ultrasonic frequency leads to an increase in attenuation which ultimately limits the useful frequency range for imaging. Doppler ultrasound can be used to image blood flow and tissue motion and to quantify this motion in terms of direction, velocity, or quantity, for instance. While the spatial resolution of ultrasonic imaging systems is quite good, the metabolic information obtained is less than that obtained using optical techniques. In addition, lack of contrast hinders the imaging of blood vessels and abnormal tissue morphologies.

In some sense then, light and ultrasound are complimentary imaging modalities. Light provides contrast in the form of metabolic information derived from hemoglobin concentration and oxygenation and ultrasound provides more than an order-of-magnitude better resolution. Because both modalities offer penetration depths of several centimeters and excellent temporal resolution, it seems feasable to combine them to obtain the advantages of both in a single imaging modality.

Several efforts have begun during the middle of the 1990s to use sound and light simultaneously. These efforts can be logically divided into several groups, depending on the way in which the modalities are combined. Two categories are true multi-modal sensing and form the subject matter of this paper. They include optoacoustic imaging, in which pulsed light generates sound which is then imaged, and various forms of ultrasound-modulated diffusive optical imaging, in which light is "tagged" with ultrasound. Several other combinations are not considered in this paper. These include sonoluminescence, in which sound generates light, and the simultaneous but independent use of two modalities. In addition, we note that there is ongoing work in the use of light and sound in therapy.

Section 2 of this review discusses optoacoustic imaging, and Section 3 discusses the modulation of diffusive light by ultrasound, variously called acousto-photonic imaging (API), ultrasound-modulated optical tomography (USMOT), and ultrasound tagging of light (UTL).

2. Optoacoustic Imaging

2.1. Optoacoustic Signal Generation

Acoustic waves generated by pulsed laser sources have been used for a variety of materials characterization, nondestructive evaluation, and sensor applications in a wide range of disciplines including photoacoustic spectroscopy [1,2], laser-based ultrasonics [3,4], and biomedical optoacoustics [5–8]. In optoacoustic imaging, a nanosecond pulsed laser is used to irradiate a tissue volume and absorption of laser energy leads to rapid heating and thermal expansion of the tissue. Broadband ultrasonic waves are subsequently launched through the thermoelastic effect and detected using ultrasonic transducers at the sample surface. The detected signals can then be processed and back-projected to give a 3-D representation of the internally absorbed electromagnetic energy distribution within the tissue.

Optoacoustic imaging takes advantage of the high optical contrast between various constituents of tissue. Hemoglobin offers strong optical contrast in the visible and near-IR region of the spectrum and makes it well-suited to imaging blood vessels or detecting developing tumors which have higher blood content than the surrounding tissue. Optoacoustic imaging maps the optical properties of tissue onto an ultrasonic wave field that is less sensitive to scattering and attenuation than the light field. It has the potential to provide substantial improvements in image resolution over other all-optical imaging modalities such as diffuse optical tomography. Additionally, optoacoustics offers advantages over conventional ultrasonic imaging. While both techniques rely on the detection of ultrasonic waves, optoacoustic imaging replaces the low ultrasonic contrast found in tumors or blood vessels with high optical contrast, and uses the ultrasonic waves to transport the optical information to the surface [9].

When a laser source interacts with an absorbing medium, some of the energy is absorbed and converted to heat. The resulting thermal expansion leads to pressure variations and launches acoustic waves. The pressure field generated by a short laser pulse in biological tissue contains information about the spatial distribution of absorbed electromagnetic radiation within the tissue. The discussion in this section will focus on the thermoelastic laser generation of acoustic waves in gases and nonviscous liquids, appropriate for most biomedical optoacoustic applications. The laser source fluence is held sufficiently low such that phase changes and associated tissue damage are avoided. Consider the one-dimensional case illustrated in Figure 2 showing a pulsed laser source illuminating a homogeneous liquid from an optically transparent media. If we assume that the optical penetration depth in the liquid is significantly larger than the thermal diffusion length on the time scale of the generation pulse, a condition known as ''thermal confinement'',

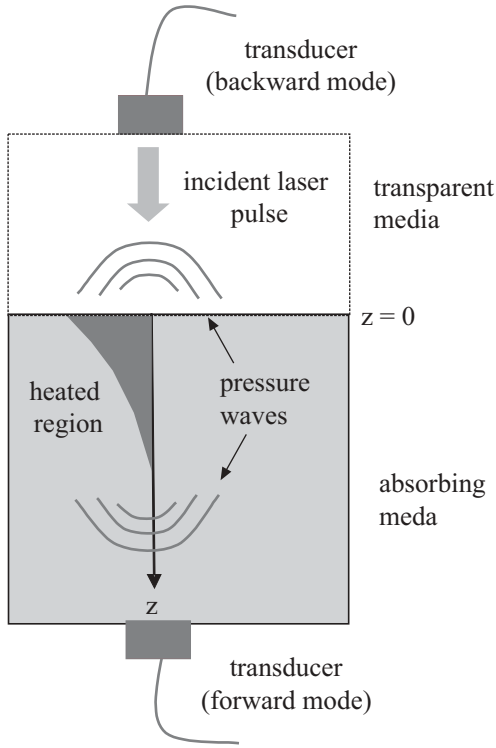

Figure 2. Schematic of optoacoustic imaging setup showing the incident laser pulse and subsequent pressure wave generation. The pressure waves can be detected in either forward or backward mode.

then thermal diffusion will have negligible effects on the resulting temperature distribution. In this case, the temperature rise within the liquid is given by:

$$\Delta T = \frac{E_a}{\rho C_p} \tag{1}$$

where E_a is the absorbed laser energy per unit volume, ρ is the density, and C_p is the heat capacity. The absorbed laser energy is determined by the incident laser fluence, F, as well as the local absorption coefficient, μ_a. For example, the temperature rise in a homogeneous liquid with an optical absorption coefficient μ_a is given by:

$$\Delta T = \frac{\mu_a F}{\rho C_p} \exp(-\mu_a z) \tag{2}$$

The laser-induced heating leads to a pressure increase in the liquid which is determined by the relative volume change ($\Delta V/V$), the thermal volume expansion coefficient (β), and the bulk modulus (B) as given below:

$$P = -B\frac{\Delta V}{V} + B\beta\Delta T \tag{3}$$

The condition of "stress confinement" is achieved if the acoustic transit time across the region of interest is long relative to the incident laser pulse width and the medium does not have time to deform during the process of heating. Referring back to Eq. (3) it can be seen that under stress confinement the first term goes to zero thus maximizing the generated pressure. Also, under stress confinement the pressure distribution is directly proportional to the temperature distribution which, in turn, is directly proportional to the absorbed laser energy distribution. The pressure distribution thus gives a convenient method of mapping the optical absorption profile within the tissue.

Laser-induced heating pressure transients propagate through the sample as illustrated in Figure 2. Optoacoustic imaging can be performed in either forward or backward detection modes corresponding to the receiving transducers on the opposite side of the sample as the illumination source and same side, respectively. Note that backward mode imaging is somewhat more difficult to implement in practice than forward mode because the laser source and receiver need to be co-located on the sample surface. This can be done by making an annular transducer such that the laser source can pass through the transducer or by designing a sensor head which allows for both optical and acoustic access to the surface. For the simple 1D case presented above, the pressure observed in the forward mode $P(fwm)$ and backward mode $P(bwm)$ can be found by solving the elastic wave equation with a thermal source term. Assuming an instantaneous heat source, the solution is given as:

$$\begin{aligned} P(fwm) &= \frac{B\beta}{2\rho C_p}\mu_a F(H(-\tau_b)\exp(\mu_a c_B \tau_b) + R_A H(\tau_b)\exp(-\mu_a c_B \tau_b)) \\ P(bwm) &= \frac{T_A B\beta}{2\rho C_p}\mu_a F H(\tau_a)\exp(-\mu_a c_B \tau_a) \end{aligned} \tag{4}$$

where H is the Heaviside step function, c_A and c_B are the acoustic wave velocities in the transparent layer and absorbing layer, $\tau_a = t + z/c_A$ and $\tau_b = t - z/c_B$, and R_A and T_A are the ultrasonic reflection and transmission coefficient between the absorbing and transparent layer. The forward and backward mode solutions have been plotted in Figure 3 for the case where the acoustic impedance of the transparent layer is less than that of the absorbing layer (i.e. R_A is negative). The origin is taken at the interface as shown in Figure 2 and the signals have been shifted such that the signal from

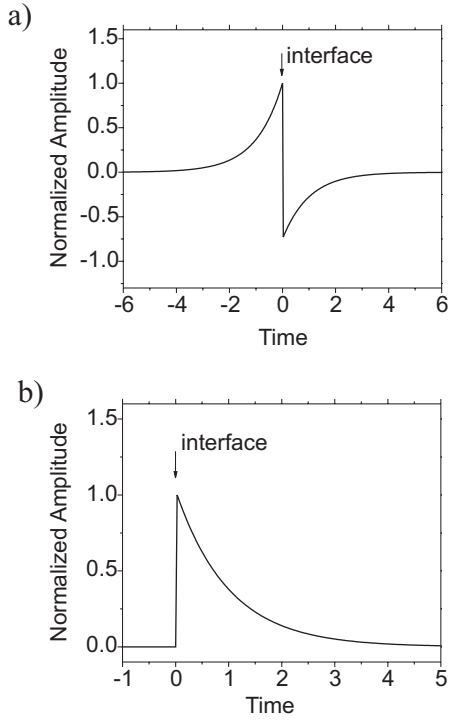

Figure 3. Theoretical optoacoustic signals generated in a homogeneous liquid and detected in a) the forward mode and b) the backward mode.

the interface arrives at $t = 0$. The time axis has been multiplied by $\mu_a c_B$. For the forward mode case the tail end of the absorbed laser pulse which penetrates furthest into the material creates an exponentially increasing signal. At the point marked *interface* on the plot there is a sign change from the acoustic reflection at the interface between the absorbing and transparent media, producing a tensile pulse. For the backward mode case the signal initially jumps to the peak corresponding to the high incident fluence near the surface and subsequently decays to zero. Note that the exponential rise (forward mode) or fall (backward mode) can be used to find the absorption coefficient in the liquid provided that the speed of sound in the liquid is known.

Optoacoustic imaging in more complex media exhibiting scattering and containing optical inhomogeneities is discussed in the literature [5,10–13]. Optoacoustic imaging can be used to determine the absorption coefficient in homogeneous media or effective absorption coefficient for optically turbid media exhibiting both attenuation and scattering. It can also be

used to image local optical inhomogeneities within the optical absorption depth. For example, consider the case of a spherical absorber of radius a (a tumor, for instance) buried within a transparent medium. The incident laser energy will be selectively absorbed by the tumor causing a local temperature rise. The following conditions are assumed: a) thermal confinement ($a \gg$ thermal diffusion length), b) stress confinement (laser pulse width $\ll a/c$), c) weak absorption such that $1/\mu_a \gg a$, and d) the acoustic properties of the tumor are identical to those of the surrounding media. Under these conditions the tumor will be uniformly heated by the laser pulse launching pressure waves as illustrated in Figure 4a. The shape of the pressure pulse has the simple form shown schematically in Figure 4b. Note that the width of the N-shaped pulse allows us to find the size of the absorber. At some detection point r, the following relations hold: $t_1 = (r-a)/c$ and $t_2 = (r+a)/c$ such that

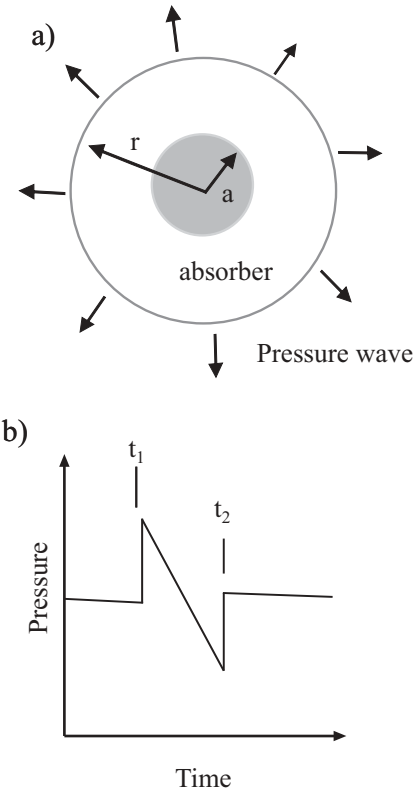

Figure 4. Schematic showing a) optoacoustic generation in a small spherical absorber and b) the pressure pulse profile.

the radius of the absorber is given by the simple relation $a = (t_2 - t_1)c/2$. In general, an optoacoustic signal will consist of the summation of the signals from the background absorption of the tissue (Figure 3) and signals from local optical inhomogeneities within the tissue (Figure 4). Arrays of detection transducers can be used to collect optoacoustic signals to create tomographic images of the optical properties of tissue. The signals are then processed (diffraction corrections may be required) and back-projected to give 2D images of the absorption profile within tissue.

2.2. Optoacoustic Imaging Applications

Photoacoustic spectroscopy has a long history and has been used to study the optical properties of a solid, liquids, and gases [1,2,13]. This technique generally makes use of the amplitude of the acoustic signal to extract information about the media while neglecting the temporal information. The relationship between the spatial distribution of absorbed laser energy and the resulting acoustic signal was studied in the late 1970s [14]. This opened up the possibility of using the temporal profile of optoacoustic signals to measure the absorption coefficient in homogeneous materials as demonstrated in 1979 [15]. The application of optoacoustic imaging in medical applications emerged in the 1990s with early work focusing on detection of absorbers buried in optically turbid media using the time-of-arrival of the acoustic transients. Optoacoustic imaging in optically turbid media required that the nature of the optical interaction to be well understood in order to account for absorption, scattering, and scattering anisotropy. A critical breakthrough in optoacoustic imaging technology came in the mid-1990s when it was realized that under the conditions of stress confinement, the acoustic signals could be used to deduce the spatial distribution of the absorption of electromagnetic radiation within tissue [16]. It was shown that the time-domain waveforms obtained in optoacoustics could be quantitatively related to the optical properties of the sample.

In the last few years there has been a substantial increase in activity in the field of optoacoustic imaging. The ability of optoacoustic imaging systems to measure optical properties within highly scattering, optically inhomogeneous media makes it an extremely promising tool for diagnostic imaging.

Optoacoustic imaging has been used to detect small tumors in breast tissue phantoms and a clinical prototype called LOIS (Laser Optoacoustic Imaging System) has recently been developed by Oraevsky *et al*. [17,18] and tested for beast cancer detection and localization *in vivo*. The system uses a Nd:YAG laser operating at 1064 nm with a 10 ns pulse width for acoustic wave generation. An array of 32 specially designed broadband piezoelectric

polymer transducers are used for detection, with the transducers arranged on an arc surface 120 mm in diameter giving a viewing angle of 120°. The system works in forward mode with an expanded laser beam (1 cm in diameter) illuminating the breast on one side and the detection transducer array on the opposite side. Images are obtained by first filtering out the low frequency signals resulting from homogeneous absorption in the background tissue and subsequently using a radial back-projection algorithm. The LOIS system was shown to be capable of detecting 2 mm blood vessels buried 7.5 cm within tissue phantoms. The depth resolution is 0.4 mm and the lateral resolution is a function of the position of the absorber relative to the array and has a typical value of about 1 mm. The authors tested the system on 5 patients *in vivo* and the LOIS system showed resolution comparable to x-ray and ultrasound images while the images obtained using the LOIS system had significantly higher contrast between tumors and surrounding tissue. A new version of the LOIS system (LOIS-2) has been developed which makes use of two laser sources for functional imaging [19]. The system uses generation laser sources at both 1064 nm and 757 nm. The spectral properties of oxygenated and deoxygenated blood are different at these two wavelengths and the optoacoustic signal amplitudes can be used to estimate the oxygen content in blood in a tumor. Initial experiments demonstrate the feasibility of using the system for noninvasive cancer diagnosis. Malignant tumors are expected to possess high concentrations of deoxyhemoglobin while benign tumors will have higher concentrations of oxyhemoglobin.

Optoacoustic systems have been proposed as monitoring devices in a number of medical applications. Viator *et al.* [20] recently presented an endoscopic optoacoustic probe to measure the depth of treatment after photodynamic therapy (PDT). In PDT treatment of esophageal cancer, the patient is given a photosensitive drug which accumulates in the cancerous region and is selectively activated by a fiber optic probe. Activation results in cell death and tissue blanching near the surface caused by the cessation of perfusion. The authors are developing optoacoustic probes to detect the depth of the treated region. Oberheide *et al.* [21] has used optoacoustic imaging for the online control of glaucoma treatment through laser cyclophotocoagulation. In this treatment, a CW laser is used to coagulate the ciliary body to decrease water production and relieve intraocular pressure in glaucoma patients. The optoacoustic imaging system serves as an online process-control tool allowing for the localization of the area of interest as well as online monitoring of tissue destruction. The authors demonstrate localization of the ciliary body in porcine and rabbit eyes. Schule *et al.* [22] proposed using optoacoustic techniques to monitor selective retinal pigment epithelium (RPE) treatment. The authors show that it is possible to detect laser-induced cell damage in RPE by monitoring the generated acoustic transients.

Optoacoustics has also been used for monitoring drug delivery and chemical concentrations in the blood. Karabutov *et al*. [23] has demonstrated the utility of optoacoustic imaging for real-time monitoring of drug and contrast agent penetration into tissue. The technique has the potential for measuring drug penetration depth as a function of time and to provide quantitative information on the concentration distribution, migration velocity, and diffusion coefficient of drugs in tissue and nails. The authors demonstrated an optoacoustic system capable detecting low concentration levels of optically absorbing or scattering-reducing solutions in the skin and differentiating drug propagation mechanisms. Zhao and Myllyla [24] have demonstrated that the optoacoustic signal generated in blood is affected by the glucose concentration thus opening up the possibility of using optoacoustics for non-invasive glucose monitoring. The authors state that the osmotic and hydrophilic properties of glucose decrease the reduced scattering coefficient of blood when dissolved glucose surrounds blood cells.

Additional optoacoustic techniques involve characterization of the skin and imaging of the vasculature. Viator *et al*. [25] have developed an optoacoustic system to determine port wine stain and epidermal melanin depth noninvasively. This research is aimed towards optimizing laser treatment of port wine stains. Hoelen [26] demonstrated three-dimensional optoacoustic imaging of blood vessels in tissue. Their system uses a pulsed laser operating at 532 nm for generation and focuses on near surface tissue imaging. They demonstrate a depth resolution of $\sim 10\ \mu$m and lateral resolution (limited by the detector diameter) of about 200 μm. Yamazaki *et al*. [27] have used the optoacoustic technique for burn diagnostics. The photoacoustic signal is used to classify burn types by studying the amplitude of the signals generated as a function of wavelength over the 500–600 nm wavelength band.

A significant technical challenge in the development of time-resolved optoacoustic imaging has been in the detection of the acoustic signals. A variety of ultrawide bandwidth, low-noise transducers have been developed and/or utilized for optoacoustic applications [6–8]. The piezoelectric polymer PVDF has been the material of choice for many applications due to the low acoustic impedance and wide bandwidth (without strong resonances). For the detection of high frequency acoustic transients, where frequency components may extend to the 100s of MHz range, piezoelectric crystals such as quartz and lithium niobate have been used. These materials exhibit low attenuation of acoustic waves at high frequencies relative to commonly available piezoceramics. Various researchers have proposed optical detection of optoacoustic transients. These techniques have potential advantages in that the optical detection systems are extremely broadband and large area optical array detectors with small element spacing may be fabricated using, for

example, diffraction gratings. Optical detection systems have been developed based on acoustically induced change in refractive index [28], etalon-based detection of acoustic waves [29], and single-point interferometry systems which are scanned over the specimen [30].

3. Modulation of Light by Ultrasound

Modulation of light by ultrasound has been studied extensively since the pioneering work of Raman and Nath beginning in the 1930s [31]. However, the use of ultrasound with light in highly scattering media dates only to the middle of the 1990s, and it remains to be fully understood and exploited for medical imaging. Because the concept of diffusive optical imaging is critical to understanding this interaction, we begin with a brief description of that field. We then discuss the concepts of mixing diffusive imaging with ultrasound and follow with a summary of work in the field since 1993.

3.1. Diffusive Optical Tomography (DOT)

It is well known that optical imaging can resolve objects down to sizes smaller than a wavelength. However, in tissue, the resolution is not determined by this fundamental physical limitation, but rather by the scattering of light away from a straight line. This can be understood by noting that we can see the large blood vessels on our hands, but the optical properties of the smaller vessels are simply averaged with those of the surrounding tissue. Fortunately, light, particularly in the red and near infrared, is not strongly absorbed by tissue. It is probable that light entering tissue will be scattered many times before being either absorbed or emitted from the surface. As a result of the scattering, the emitted light can be considered to have traveled from the source to the receiver *via* many paths, each having a different length. Typical path lengths are as much as 6 or 10 times the shortest, straight-line path. These long paths increase the opportunity for absorption, and the diversity of their lengths creates a diversity in transit time. The presence of any inhomogeneity in the tissue will alter these paths, and thus change the amplitude and temporal behavior of the received light. The propagation of light in these circumstances follows the radiative transport equation and in the diffusion approximation, the fluence rate, ϕ, varies according to the photon diffusion equation;

$$\phi = \frac{dF}{dt} \quad \nabla \frac{cD}{n} \nabla \phi - \frac{\partial \phi}{\partial t} - \frac{\mu_a c}{n} \phi = 0 \tag{5}$$

where the diffusivity is given by

$$D = \frac{1}{3(\mu_s' + \mu_a)}$$

$\mu_s' = \mu_s(1-g)$, is the transport scattering coefficient, μ_s is the scattering coefficient, g is the anisotropy, μ_a is the absorption coefficient, n is the index of refraction of the background medium, c is the speed of light in vacuum, and t is time.

By using multiple sources and receivers on a surface, it is possible to compute spatial behavior of the optical parameters μ_s' and μ_a throughout the contained volume. In essence, this is a near-field imaging problem, and the resolution degrades as the depth of the features to be resolved increases. The light may be CW, pulsed, or modulated at a frequency typically greater than 100 MHz. This type of measurement, combined with the implied inverse problem called diffusive optical tomography (DOT), is the subject of hundreds of papers since the first images were reported in 1992 [32]. An excellent review is presented in [33].

3.2. Ultrasound Modulation of Diffuse Light

The use of ultrasound to enhance the resolution of DOT is the subject of recent research. Figure 5 shows the general experimental configuration. Diffusive light is introduced into the sample in such a way that some of it will pass through the focus of the ultrasound, and a receiver collects energy from the original source, including the portion modulated by the ultrasound. In

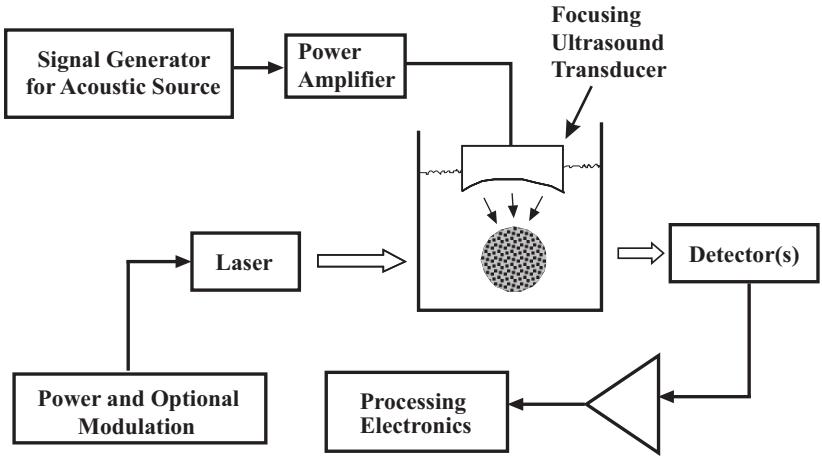

Figure 5. General layout for interaction of diffusive optical waves with ultrasound.

the work of Raman and Nath, the medium was optically transparent, and the problem is clearly defined as the interaction of a well-defined optical wave with a medium having an index of refraction modulated by the ultrasound wave. The strong scattering complicates the analysis, first because the light travels only a short distance (often less than the acoustic wavelength), before being scattered into a new direction, and secondly because the scattering particles themselves may be moved by the ultrasound wave.

At a given receiver location, the field amplitude of the light will be the sum of contributions over all paths. This sum will result in a speckle pattern, having a mean value determined by the solution of the photon diffusion equation above. If the light source has sufficient coherence, this speckle pattern will have strong peaks and nulls resulting from the different phases of the contributions to the sum. Introduction of the ultrasound will produce a modulation of the speckle pattern because of changes in the index of refraction of the medium between scattering events, and because of motion of the scattering particles. Because of the random location of scatterers and random directions of propagation of the light, the phase changes will be unpredictable, leading to random modulation of the speckle with respect to the acoustic source. The mean value of the irradiance can be determined by solving the photon diffusion equation with the scatterer concentration and pressure, and thus μ_a, μ_s' and n, varying at the acoustic frequency as the medium is compressed and rarefied. The signals are generally weak.

In the Raman-Nath effect, the interaction of the light with sound is enhanced when the changes in frequency and wavenumber of the light wave are equal to the acoustic frequency and wavenumber. In the case of the wave vector, most of the change results from the change of direction through an angle θ. Thus,

$$\delta f_{opt} = f_{acoustic} \quad \delta k_{opt} \approx k_{opt} \sin\theta = k_{acoustic} \tag{6}$$

If the interaction length is short, in fact, it does not make much difference whether the Bragg condition, expressed in Equation 6, is satisfied or not. If the interaction length is greater, and the Bragg condition is satisfied, then contributions to the shifted light wave generated at various points across the sound path are coherently added, and the effect is enhanced, and the effect on other orders is decreased. Satisfying the Bragg condition is possible because the frequency and the wave vector for ultrasound are both much smaller than those of the light as shown in Figure 6. The angle of the frequency-shifted wave is determined so that the wave vector condition is satisfied, as shown in Figure 7.

If the interaction of sound with a diffusive wave were analogous to the Raman–Nath effect, we would get a frequency-shifted diffusive wave. The acoustic wave would change the optical properties which determine the

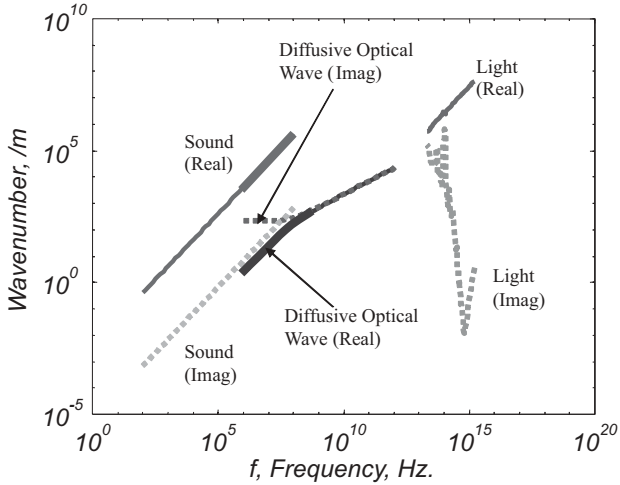

Figure 6. Dispersion curves for sound, light, and diffusive optical waves. The data are the same as in Figure 1, but the real and imaginary parts of the wavenumber are plotted on the ordinate. The wider line for the diffusive optical wave shows the useful range of these waves. Beyond about 1 GHz, the imaginary part of the wavenumber becomes too large to provide useful penetration of tissue. The wider line for the sound wave shows the range of ultrasound wavelengths useful for this application. Below about 2 MHz, they will not provide the desired resolution enhancement.

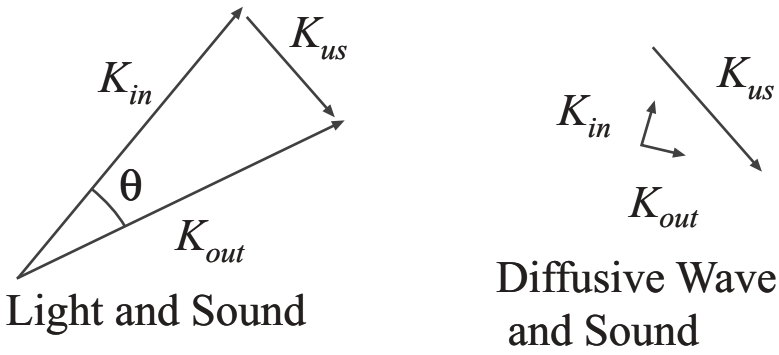

Figure 7. Matching wave vectors for interaction of light and sound.

wave-number of the diffusive wave. However, the frequency and wave vector matching can not be achieved in this case, because for all useful combinations, the frequency and wavenumber of the ultrasound waves are larger than those of the diffusive wave, as shown in Figure 6. Thus the attempt to achieve both conditions fails as shown on the right side of Figure 7. The only

way to satisfy the Bragg condition would be to use higher frequency diffusive waves (impractical because of their absorption), or lower frequency ultrasound (undesirable because we are relying on the ultrasound to provide our spatial resolution, which the low frequencies would not do). The broad lines in Figure 6 show the range of useful combinations of ultrasound and diffusive waves, making it clear that the Equations 6 can not be satisfied. The wavenumbers of diffusive waves have a large imaginary part, so even if the real parts matched, the match would not be complete. Thus the analogy of coherent Bragg scattering in diffusive waves, which would be spatially coherent and would occur regardless of the coherence of the light source, is predicted to be weak, in agreement with experiments. The next strongest effect, modulation of the speckle, has the disadvantage of not being spatially coherent.

Detection of the modulated light can be accomplished by using a large detector and long time averages to detect variations in the mean, or by using a number of small detectors, ignoring the phase and averaging the amplitude of the acoustic modulation of the light. In either case, imaging can be accomplished by using the ultrasound modulated light as a ''virtual source'' of diffusive waves at the modulation frequency, or by moving the ultrasound source throughout the volume of interest and mapping changes in the resulting signal.

3.3. Imaging Applications of Ultrasonic Modulation of Diffusive Light

The first report of mixing of diffusive waves with ultrasound appeared in 1993 [34,35], using focused, pulsed ultrasound at 1 MHz, with a CW argon ion laser and a PIN detector. Closely following this work were papers by two other groups [36,37–41]. The latter group demonstrated what they called ultrasound modulated optical tomography (USMOT), using CW ultrasound, CW light and a photomultiplier tube. It was believed that the modulation occurred in going through the focus of the ultrasound beam, and that this focus could be considered a nearly point source of diffusive light at the modulation frequency. This group also imaged buried absorbing objects in dense media by scanning the ultrasound [42,43]. DiMarzio's group [44,45] used ultrasound with a modulated laser source to produce higher frequency DOT waves and computed the point spread function based on the variations in μ_s', μ_a and n with the ultrasound. By varying the ultrasound frequency and noting that at higher frequencies the signal decreased, the authors suggested that the effect was mostly a result of particle motion and that the particles were less able to follow the acoustic wave at higher frequencies [46]. At about the same time, in experiments in weakly-scattering media, other groups reported signals which they attributed to modulation of the index of refraction [47,48].

To improve the ability to image in three dimensions, Wang used a frequency-swept ultrasound source, so that the frequency information could be used to resolve position along the ultrasound beam [49,50].

A major breakthrough occurred in the recognition that ultrasound-induced changes in the speckle pattern were random, and Boccara's group introduced the idea of collecting data on a charge-coupled device (CCD) camera, using a laser synchronized with the ultrasound at several different phases, followed by averaging over the CCD pixels of the magnitude of the variation [51–53].

Subsequently, Wang and Yao combined the speckle imaging with their swept-frequency technique [54–56], and another group began studies of image quality using a tunable NIR laser and a wide range of ultrasound frequencies [57], using low-frequency AM modulation of the ultrasound to improve the SNR [58].

In 2000, several new investigations into the basic mechanism were undertaken. Our own group began to investigate detailed models including realistic ultrasound beam profiles [59]. Wang and Yao developed an analytical model [60,61] and a Monte-Carlo model [62], indicating that the relative importance of particle motion and index variation depended upon the relationship between the optical mean free path in the scattering medium and the acoustic wavelength. Specifically, in water solution, modulation of the index of refraction becomes increasingly more important in comparison to motion of the scatterers when the scattering mean free path increases relative to the acoustic wavelength. Our group combined an ultrasound wave model of pressure and particle motion with a model based on a frequency-domain Monte-Carlo approach [63,64], which is currently being used to analyze the effect of laser modulation.

Boccara's group has developed instrumentation for simultaneous measurement of optical and acoustic contrast [65,66], and has reported measurements at the second harmonic of the acoustic frequency, with improvements in spatial resolution [67].

Although acousto-photonic signals are weak and complicated by speckle variations, the utility of optical imaging for spectroscopy and ultrasound imaging for spatial resolution encourages continuing research in this field.

4. Summary

Light and ultrasound have both established themselves as viable medical imaging techniques. In many ways, they offer complimentary capabilities. An obvious concept would be to use both types of instrumentation in diagnosis. Such an approach would provide the spectroscopic ability of light to

detect endogenous and exogenous chromophores, and the high resolution images of tissue with contrasting acoustic properties provided by ultrasound. However, to obtain high resolution images of the optical properties, it is necessary to consider true multi-modal imaging, where the light and sound are combined in a single technique. We have described here the two most common of these techniques.

References

1. Tam, A.C., 1986, Applications of photoacoustic sensing techniques: Rev. Mod. Phys., v. 58, no. 2, p. 381–431.
2. Zarov V.P. and Letokhov, V.S., 1984, Laser Optoacoustic Spectroscopy, Springer Verlag, New York.
3. Hutchins, D.A., 1986, Mechanisms of pulsed photoacoustic generation: Can. J. Phys., v. 64, p. 1247–1264.
4. Scruby, C.E. and Drain, L.E., 1990, Laser Ultrasonics, Techniques and Applications, Adam Hilger, New York.
5. Oraevsky, A.A. and Karabutov, A.A., 2002, Time resolved detection of optoacoustic profiles for measurement of optical energy distribution in tissues, in Tuchin, V.V. (ed.), Handbook of Optical Biomedical Diagnostics: SPIE Press, WA, p. 585–646.
6. Oraevsky, A.A., ed., 2000, Biomedical Optoacoustics: Proc. SPIE, v. 3916.
7. Oraevsky, A.A., ed., 2001, Biomedical Optoacoustics II: Proc. SPIE, v. 4256.
8. Oraevsky, A.A., ed., 2002, Biomedical Optoacoustics III: Proc. SPIE, v. 4618.
9. Esenaliev, R.O., Karabutov, A.A., and Oraevsky, A.A., 1999, Sensitivity of laser optoacoustic imaging in detection of small deeply imbedded tumors: IEEE J. Selected Topics in Quant. Elect., v. 5, no. 4, p. 981–988.
10. Karabutov, A.A., Podymova, N.B., and Letokhov, V.S., 1996, Time-resolved optoacoustic tomography of inhomogeneous media: Appl. Phys. B, v. 63, p. 545–563.
11. Paltauf, G., Schmidt-Kloiber, H., and Frenz, M., 1998, Photoacoustic waves excited in liquids by fiber transmitted laser pulses: J. Acoust. Soc. Am., v. 104, no. 2, p. 890–897.
12. Hoelen, C.G.A. and de Mul, F.F.M., 1999, A new theoretical approach to photoacoustic signal generation: J. Acoust. Soc. Am., v. 106, no. 2, p. 695–706.
13. Gusev, V.E. and Karabutov, A.A., 1993, Laser Optoacoustics, AIP, New York.
14. Burmistrova, L.L., Karabutov, A.A., Portnyagin, A.I., Rudenko, O.V., and Cherepetskaya, E.B., 1978, Method of transfer function in problems of thermooptical sound generation: Sov. Phys. Acoust., v. 24, no. 5, p. 369–373.
15. Karabutov, A.A., Portnyagin, A.I., Rudenko, O.V., and Cherepetskaya, E.B., 1979, Nonlinear transformation of thermooptically excited acoustic pulses: J. Tech. Phys. Lett., v. 5, no. 6, p. 328–332.
16. Oraevsky, A.A., Jacques, S.L., and Tittel, F.K., 1993, Measurement of tissue optical properties by time resolved detection of laser-induced stress waves: Proc. SPIE, v. 1882, p. 86–101.
17. Andreev, V.G., Karabutov, A.A., Solomatin, S.V., Savateeva, E.V., Aleinikov, V., Zhulina, Y.V., Fleming, R.D., and Oraevsky, A.A., 2000, Optoacoustic imaging of breast cancer with arc-array transducer: Proc. SPIE, v. 3916, p. 36–47.
18. Oraevsky, A.A., Karabutov, A.A., Solomatin, S.V., Savateeva, E.V., Andreev, V.G., Gatalica, Z., Singh, H., and Fleming, R.D., 2001, Laser optoacoustic imaging of breast cancer *in vivo*: Proc. SPIE, v. 4256, p. 6–15.

19. Oraevsky, A.A., Savateeva, E.V., Solomatin, S.V., Karabutov, A.A., Andreev, V.G., Gatalica, Z., Khamapirad, T., and Henrichs, P.M., 2002, Optoacoustic imaging of blood for visualization and diagnostics of breast cancer: Proc. SPIE, v. 4618, p. 81–94.
20. Viator, J.A., Paltauf, G., Jacques, S.L., and Prahl, S.A., 2001, Design and testing of an endoscope photoacoustic probe for determination of treatment depth after photodynamic therapy: Proc. SPIE, v. 4256, p. 16–27.
21. Oberheide, U., Jansen, B., Bruder, I., Labatschowski, H., and Welling, H., 2001, Optoacoustic online control for laser cyclophotocoagulation: Proc. SPIE, v. 4256, p. 53–60.
22. Schule, G., Joachimmeyer, E., Framme, C., Roider, J., Birngruber, R., and Brinkmann, R., 2001, Optoacoustic control system for selective treatment of the retinal pigment epithelium: Proc. SPIE, v. 4256, p. 71–76.
23. Karabutov, A.A., Savateeva, E.V., and Oraevsky, A.A., 2001, Real time monitoring of substance penetration in tissue: Proc. SPIE, v. 4256, p. 61–70.
24. Zhao, Z. and Myllyla, R., 2001, Photoacoustic determination of glucose concentration in whole blood using a near-infrared laser diode: Proc. SPIE, v. 4256, p. 77–83 .
25. Viator, J.A., Au, G., Choi, B., and Nelson, J.S., 2002, Design limitations of a photoacoustic probe for port wine stain depth determination: Proc. SPIE, v. 4618, p. 7–15.
26. Hoelen, C.G.A., de Mul, F.F.M., Pongers, R., and Dekker, A., 1998, Three-dimensional photoacoustic imaging of blood vessels in tissue: Opt. Lett., v. 23, no. 8, p. 648–650.
27. Yamazaki, M., Sato, S., Saito, D., Fujita, M., Okada, Y., Kikuchi, M., Ashida, H., and Obara, M., 2002, Photoacoustic signal measurement for burned skins in the spectral range of 500–650 nm: experiment with rat burn models: Proc. SPIE, v. 4618, p. 16–21.
28. Paltauf, G., Schmidt-Kloiber, H., Kostli, K.P., and Frenz, M., 1999, Optical methods for two-dimensional ultrasonic detection: Appl. Phys. Lett., v. 75, no. 8, p. 1048–1050.
29. Beard, P.C. and Mills, T.N., 2001, 2D line scan photoacoustic imaging of absorbers in scattering tissue: SPIE, v. 4256, p. 34–42.
30. Hamilton, J.D. and O'Donnell, M., 1998, High frequency ultrasound imaging with optical arrays: IEEE Trans. Ultra., Ferroelect., and Freq. Contr., v. 45, no. 1, p. 216–235.
31. Raman, C.V., *et al*., 1966, Proc. Indian Acad. Sci. A: Ann. Phys. (Paris), v. 17, p. 103.
32. O'Leary, M.A., Boas, D.A., Chance, B., and Yodh, A.G., 1992, Refraction of diffusive photon density waves: Phys. Rev. Lett., v. 69, p. 2658.
33. Boas, D.A., Brooks, D.H., Miller E.L., DiMarzio, C.A., Kilmer, M., Gaudette, R.J., and Zhang, Q., 2001, Imaging the body with diffuse optical tomography: IEEE Signal Process. Mag., November 2001, v. 18, no. 6, p. 57–75.
34. Marks, F.A., Tomlinson, H.W., and Brooksby, G.W., 1993, A comprehensive approach to breast cancer detection using light: photon localization by ultrasound modulation and tissue characterization by spectral discrimination: Proc. SPIE, v. 1888, p. 500–510.
35. Brooksby, G.W. and Murray Penney, C., 1995, Measurement of ultrasonically modulated scattered light for imaging in turbid media: SPIE, v. 2389, p. 564–570.
36. Leutz, W. and Maret, G., 1995, Ultrasonic modulation of multiply scattered light: Physica B, v. 204, p. 14–19.
37. Wang, L., Zhao, X., and Jacques, S.L., 1995, Ultrasound-modulated optical tomography for thick tissue imaging: Proc. SPIE, v. 2626, p. 237–248.
38. Wang, L.-H., Zhao, X.-M., and Jacques, S.L., 1995, Ultrasound-modulated optical tomography for thick tissue imaging: Proc. Soc. Photo-Opt. Instrum. Eng., v. 2626, p. 237–248.
39. Wang, L.-H., Zhao, X.-M., and Jacques, S.L., 1996, Ultrasound-modulated optical tomography for dense turbid media: Proc. Soc. Photo-Opt. Instrum. Eng., v. 2676, p. 91–102.
40. Wang, L.-H., Zhao, X.-M., and Jacques, S.L., 1996, Ultrasound-modulated (acousto-) optical tomography: Proc. Adv. Opt. Imaging Photon Migration, p. 325–327.

41. Wang, L.-H. and Zhao, X.-M., 1997, Ultrasonic modulation of diffuse light in turbid media: Proc. Soc. Photo-Opt. Instrum. Eng., v. 2979, 24–35.
42. Wang, L. and Zhao, X., 1997, Ultrasound-modulated optical tomography of absorbing objects buried in dense tissue-simulating turbid media: Appl. Opt., v. 36, no. 28, p. 7277–7282.
43. Wang, L.-H., 1998, Ultrasonic modulation of scattered light in turbid media and a potential novel tomography in biomedicine: Photochem. and Photobiol., v. 67, p. 41–49.
44. DiMarzio, C.A. and Gaudette, T.J., 1998, Point-spread functions for acousto-photonic imaging, presented at CLEO 98, San Francisco, CA, May 1998, with a summary published in Conference on Lasers and Electro-Optics (CLEO/US), OSA Technical Digest Series, Optical Society of America, Washington, DC.
45. Gaudette, T.J., Townsend, D.J., and DiMarzio, C.A., 1999, Interaction of diffusive waves and ultrasound: Subsurface Sensors Appl., Proc. SPIE, v. 3752, p. 83–89.
46. DiMarzio, C.A., Gaudette, R.J., and Gaudette, T.J., 1999, A new imaging technique combining diffusive photon density waves and focused ultrasound: Optical Tomography and Spectroscopy of Tissue III, Proc. SPIE, v. 3597, p. 376–384.
47. Hisaka, M., Sugiura, T., and Kawata, S., 1999, Ultrasound-assisted optical reflectometry in highly scattering media: Japanese J. of Appl. Phys., Part 2: Letters, v. 38, p. L1478–L1481.
48. Hisaka, M., Sugiura, T., and Kawata, S., 1999, Ultrasound-assisted optical measurement for observation inside the scattering medium: Proc. SPIE, v. 3740, p. 146–149.
49. Wang, L.-H. and Ku, G., 1998, Frequency-swept ultrasound-modulated optical tomography of scattering media: Opt. Lett., v. 23, p. 975–977.
50. Wang, L.V., Ku, G., and Shen, Q., 1999, Sound and light in turbid media: Proc. SPIE, v. 3601, p. 238–247.
51. Leveque, S., Boccara, A.C., Lebec, M., and Saint-Jalmes, H., 1999, Ultrasonic tagging of photons paths in scattering media: parallel speckle modulation processing: Opt. Lett., v. 24, p. 181–183.
52. Leveque, S., Boccara, A.C., Lebec, M., and Saint-Jalmes, H., 1999, Ultrasonic tagging of photon paths in scattering media: parallel speckle modulation processing: Opt. Soc. Amer., v. 24, no. 3, p. 181–183.
53. Leveque, S., Boccara, A.C., Beaurepaire, E., Dubois, A., Lebec, M., and Saint-Jalmes, H., 1999, Biological tissues imaged by tagging photon paths with ultrasound: Proc. SPIE, v. 3597, p. 694–701.
54. Wang, L.V. and Yao, G., 2000, Two-dimensional tissue imaging by use of parallel detection of ultrasound-modulated laser speckles: Proc. SPIE, v. 3916, p. 140–146.
55. Wang, L.V. and Yao, G., 2001, Ultrasound-modulated laser tomography: Proc. SPIE, v. 4241, p. 1–5.
56. Yao, G., Jiao, S.-L., and Wang, L.-H., 2000, Frequency-swept ultrasound-modulated optical tomography in biological tissue by use of parallel detection: Opt. Lett., v. 25, p. 734–736.
57. Yao, Y., Xing, D., and He, Y., 2000, Ultrasound-modulated optical tomography with real-time FFT: Proc. SPIE, v. 4160, p. 163–169.
58. Yao, Y. and Xing, D., 2001, Optical tomography with amplitude-modulation ultrasound: Proc. SPIE, v. 4250, p. 508–513.
59. Townsend, D.J., Stott, J.J., Roy, R.A., and DiMarzio, C.A., 2000, Ultrasound Modulation of Diffusive Optical Waves for Medical Imaging: ASME/ICEME, Proceedings ASME, International Mechanical Engineering Congress, Orlando, FL, Nov. 2000.
60. Yao, G. and Wang, L.-H., 2000, Theoretical and experimental studies of ultrasound-modulated optical tomography in biological tissue: Appl. Opt., v. 39, p. 659–664.

61. Wang, L.-H., 2001, Mechanisms of ultrasonic modulation of multiply scattered coherent light: an analytic model: Phys. Rev. Lett., v. 87, no. 043903, p. 1–4.
62. Wang, L.-H., 2001, Mechanisms of ultrasonic modulation of multiply scattered coherent light: a Monte Carlo model: Opt. Lett., v. 26, p. 1191–1193.
63. Manneville, S., Roy, R.A., DiMarzio, C.C., and Boas, D.A., 2001, A model for the ultrasonic modulation of optical path in acousto-photonic imaging: J. Acoust. Soc. Am., v. 110, no. 5 pt. 2, p. 2735.
64. Nieva, A., Manneville, S., Boas, D.A., Roy, R., and DiMarzio, C.A., 2002, Monte Carlo simulations in acousto-photonic imaging: OSA Spring Topical Meeting on Biomedical Optics (Miami), Digest published by the Optical Society of America, Washington, DC.
65. Selb, J., Leveque-Fort, S., Pottier, L., and Boccara, A.C., 2001, Setup for simultaneous imaging of optical and acoustic contrasts in biological tissues: Proc. SPIE, v. 4256, p. 200–207.
66. Selb, J., Pottier, L., Leveque-Fort, S., and Boccara, A.C., 2001, Dedicated acoustic/acousto-optic imaging system: Proc. SPIE, v. 4434, p. 89–95.
67. Selb, J., Pottier, L., and Boccara, A.C., 2002, Nonlinear effects in acousto-optic imaging: Opt. Lett., v. 27, no. 11, p. 918–920.